Intensity spiral patterns in a semiconductor microresonator

Ye. Larionova,[1,*] O. Egorov,[2] E. Cabrera-Granado,[3] and A. Esteban-Martin[4]
[1]*Physikalisch-Technische Bundesanstalt, 38116 Braunschweig, Germany*
[2]*Institut für Festkörpertheorie und Theoretische Optik, Friedrich-Schiller Universität, Max-Wien-Platz 1, Jena, D-07743, Germany*
[3]*Departamento Optica, Facultad de C.C. Fisicas, Universidad Complutense, 28040 Madrid, Spain*
[4]*Departament D'Òptica, Universitat de València, València, Spain*
(Received 10 February 2005; revised manuscript received 23 May 2005; published 30 September 2005)

Spiral waves appear frequently in nature. They have been studied, e.g., in hydrodynamic systems, chemical reactions, and in a large variety of biological and physical systems [Grill *et al.*, Phys. Rev. Lett. **75**, 3368 (1995); Goryachev and Kapral, Phys. Rev. Lett. **76**, 1619 (1996)]. In contrast to chemical and hydrodynamic processes where the field amplitude exhibits the spiral patterns (intensity spirals), in optics the spiral structures relate generally to the phase structure of the optical field (so-called "optical vortices" [Lugiato *et al.*, Adv. At., Mol., Opt. Phys. **40**, 229 (1999); Arecchi *et al.*, Phys. Rep. **318**, 1 (1999); Weiss *et al.*, Appl. Phys. B:Lasers Opt. **B68**, 151 (1999)]). Thus the question arises whether amplitude spiral patterns can exist also in optics. In [Lodahl *et al.*, Phys. Rev. Lett. **85**, 4506 (2000)] the existence of such spiral patterns in optics was theoretically predicted. Experimentally, intensity spiral patterns were shown to exist in an optical feedback system with radially symmetric excitation intensity [Huneus *et al.*, Appl. Phys. B:Lasers Opt. **B76**, 191 (2000)]. We show here that such spiral patterns occur in a widely studied system, the semiconductor microcavity. The pattern formation is influenced here by the phase- as well as the intensity structure of the exciting light field.

DOI: 10.1103/PhysRevA.72.033825 PACS number(s): 42.65.Sf, 47.54.+r

I. INTRODUCTION

In [1] it was theoretically predicted that at least in one optical system, the internally pumped optical parametric oscillator (an intracavity $\chi^{(2)}$-mediated nonlinear interaction), intensity spiral patterns could exist, even in the case of excitation by a homogeneous field with a plane wave front.

The prediction [1] has not yet been demonstrated in an optical experiment. However, the existence of intensity spiral patterns was shown for a single-mirror feedback system with atomic nonlinearity [2]. There the Gaussian intensity distribution of the exciting field creates, through a refractive index nonlinearity, a wave front curvature aiding the existence of spiral patterns. The spiral patterns are supported here by the intensity distribution of the excitation. It was also shown that they can be influenced by the wave front curvature of the exciting field.

Spiral patterns mirror a spatial modulational instability (stripe pattern). In fact, a spiral is topologically equivalent to a stripe pattern with a defect. Thus one would expect the existence of spirals near such a modulational instability. A distribution of the excitation of circular symmetry can then conceivably bend the stripe pattern into circular shape, i.e., form target patterns or spirals.

In a fluid picture of resonator optics [3], phase- and amplitude gradients correspond to flow velocity and pressure gradients, respectively. Both lead to a drift of optical structures. Drift in radially symmetric gradients can be radially outward/inward (e.g., for target patterns) or can have the form of rotating spirals. Both cases were observed in [2].

We find here that in a nonlinear resonator, a semiconductor microcavity, spirals can also exist. Phase- and intensity distribution of the exciting light field both influence the spiral patterns.

II. EXPERIMENT

The semiconductor resonator used for the experiments consists of flat Bragg mirrors of about 99.8% reflectivity, with 18 $GaAs/Ga_{0.5}Al_{0.5}As$ quantum wells between them. The optical resonator length is about 3 μm so that with a diameter of the illuminating beam of $\sim$45 μm, as used experimentally, a Fresnel number of $\sim$1000 is excited, sufficient for complex structure to form. Such resonators show optical bistability when driven by a coherent field [4] so that they can support spatial solitons, which coexist with a plane wave structure and are thus possibly useful as information carriers. This system has been shown experimentally and theoretically to support hexagonal patterns and bright and dark solitons, which are now under study theoretically and experimentally [5–8]. The experimental arrangement is essentially the same as used for the observation of solitons in [9]. Light of wavelengths near the semiconductor band edge (860 nm), generated by a continuous $Ti:Al_2O_3$ laser, illuminates the semiconductor sample (Fig. 1) through a mechanical chopper for durations of a few μs to limit thermal phenomena. The illumination is repeated at a rate of 1 kHz. Observations are made in reflection because the sample substrate is absorbing at the wavelengths used. The light reflected from the sample is imaged onto a charge coupled device camera for recording two-dimensional images. A fast intensity modulator, placed in front of the camera and trig-

*Email address: yevgeniya.larionova@ptb.de

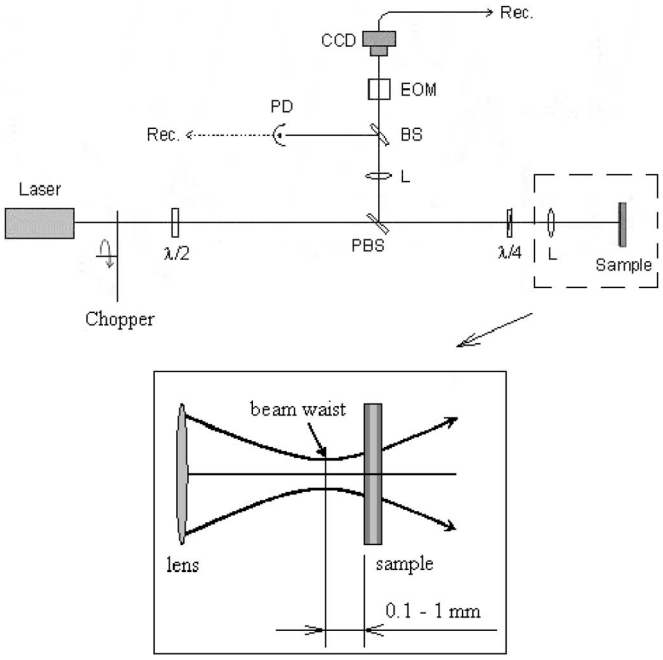

FIG. 1. Experimental setup. PBS: polarizer beam splitter, λ/2: halfwave plate, λ/4: quarterwave plate, L: lens, BS: beam splitter, EOM: electro-optical modulator, PD: photodiode, to follow intensity in time in certain points of the patterns. Inset shows the arrangement of the sample in the exciting field. Beam waist is 45 μm full width at half maximum in intensity.

gered with a variable delay with respect to the start of the illumination, allows one to take snapshots with exposure times down to a few ns. The difference to [9] is that here a phase gradient of the incident Gaussian beam was used. Whereas solitons exist in plane wave illumination, existence of spirals requires a phase gradient, as shown below. Experimentally the phase gradient is produced by shifting the resonator sample by several 100 μm beyond the beam waist behind the focusing lens (Fig. 1, inset). In this case the beam waist lies between the lens and the sample, and the Gaussian beam on the sample surface has a finite wave front curvature (which we define as positive). Figure 2 shows typical snapshots of intensity spiral patterns observed in the transverse intensity profile of the reflected light. The spirals have one

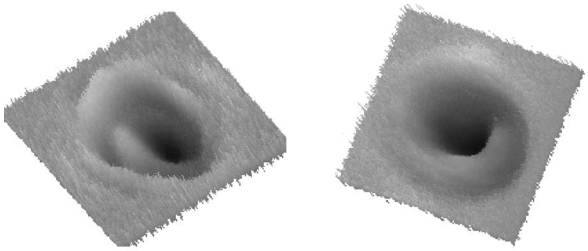

FIG. 2. Right- and left-handed intensity spiral patterns observed experimentally. Parameters: (a) wavelength of the incident light λ = 862 nm, intensity on the sample I = 14 kW/cm^2, sample position is 500 μm beyond beam waist; and (b) λ = 878 nm, I = 18 kW/cm^2, sample position is 600 μm beyond the beam waist.

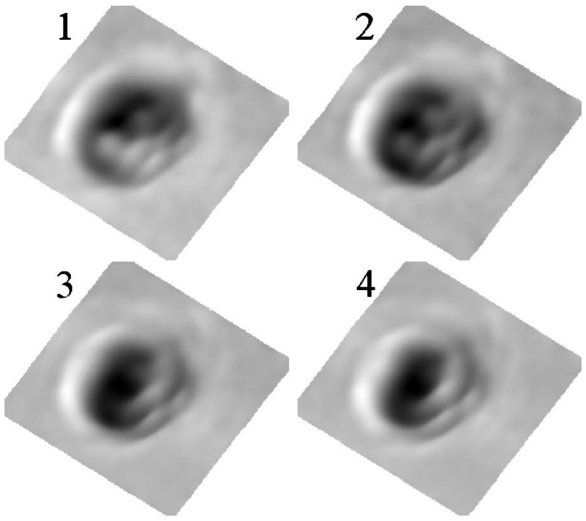

FIG. 3. Snapshots of spiral formation made experimentally during the first microsecond of illumination. λ = 862 nm, I = 14 kW/cm^2, sample position is 500 μm beyond the beam waist. Time between snapshots is ~0.2 μs.

arm and occur left- and right-handed. The spiral patterns form spontaneously from spot-stripe structures in the switched area (Fig. 3) during the illumination. During the illumination period the spirals form, develop, and can disappear. Although the duration of illumination is kept short (6 to 7 μs) to avoid unnecessary heating, at large enough intensity of the incident light the heating of the semiconductor material becomes noticeable. One of the temperature effects is the change in the semiconductor cavity detuning [10]. A change of linear refractive index of the semiconductor material with temperature and optical length changes shifts the cavity resonance. The corresponding changes in detuning are the main reason for the temporal changes of the spiral patterns.

The fact that a wave front curvature is necessary for spirals to exist (see also results of model calculations) shows up in the result that the spirals can be observed only within a certain distance range from the beam waist (within the Rayleigh range). Spirals were not found for distances less than 100 μm beyond the beam waist of the illuminating light (radius of wave front curvature for this distance is approximately 150 mm). The maximum distance for existence of spirals is around 1 mm from the beam waist which corresponds to ~15 mm of radius of the wave front curvature. At larger distances from the beam waist the exciting intensity is too low to form spirals since the beam diverges with propagation. For the radii of the wave front curvature outside this range (see also theoretical model results) the spiral patterns are unstable and disappear, therefore, quickly. Experimenting with negative phase curvature of the incident beam (at a position of the sample between the focusing lens and the beam waist) showed no spiral patterns.

III. MODEL

For the analysis a model was used which was shown to be adequate for a semiconductor resonator [11]. The set of nor-

malized equations for the intracavity field E and the carrier density N is

$$\frac{\partial E}{\partial t} = -(1+i\theta)E + iD_E\nabla_\perp^2 E + E_h - i\chi(N-1)E,$$

$$\frac{\partial N}{\partial t} = -\delta_N N - \beta N^2 + D_N\nabla_\perp^2 N - (N-1)|E|^2, \qquad (1)$$

where $\theta=\tau_{ph}(\omega_{res}-\omega_0)$ is the cavity detuning parameter, ω_{res},ω_0 are the resonance and exciting field frequencies, respectively, $\tau_{ph}(\sim 4$ ps) is the photon lifetime in the resonator without absorption, D_E,D_N are diffraction and diffusion coefficients, $E_h=E_{ext}[\sqrt{1-\rho_u^2}/(1-\rho_u\rho_l)]$ is the holding beam amplitude, where E_{ext} is the illuminating field amplitude incident on the input (upper) mirror, ρ_u,ρ_l are the reflectivity coefficients of upper and lower mirror, respectively, χ is the complex nonlinearity coefficient, δ_N is the ratio of the photon lifetime in the resonator to the carrier recombination time, and β is the radiative recombination coefficient. The following parameters are used for calculations: $\chi=16.1+7.66i$, $D_E=6.53$, $D_N=2.32\times10^{-3}$, $\delta_N=5.8\times10^{-4}$, and $\beta=3.8\times10^{-4}$. N is normalized to the carrier density at transparency N_0. The transverse coordinates are given in μm. Time is normalized to τ_{ph}; E, E_{ext} are normalized to $\sqrt{\hbar N_0 L\omega_0/\varepsilon_0\nu\,\mathrm{Im}(\chi)(1-\rho_u\rho_l)}$; $\hbar$, and ε_0 are the Plank constant and vacuum susceptibility, respectively. ν is the light velocity in matter and L is the thickness of the quantum well stack.

A Gaussian-shaped illuminating beam was used for the numerical simulations:

$$E_h(r,z) = E_s(z)e^{-r^2/W_s(z)^2+i(k/2)r^2/R_s(z)},$$

where E_s is the maximum amplitude of the illuminating light on the sample, W_s is the amplitude radius of the illuminating light, R_s is the radius of wave front curvature of the illuminating light on the sample, and r is the transverse coordinate.

In agreement with the experimental results, in simulations with spiral initial conditions stable intensity spiral patterns [Fig. 4(a)] are found for curvatures corresponding to the position of the sample beyond the beam waist. This indicates that positive wave front curvature is important for the spiral formation. Therefore we used initially a relatively wide Gaussian-shaped beam ($W_s=200$ μm) for numerical simulations to investigate the influence of wave front curvature. The simulations show a rotation of the spiral patterns [Fig. 4(b)]. It is well-known that a uniform phase gradient induces a drift motion in an infinitely extended system [12,13]. Here, in contrast, the drift velocity is directed radially in or out, depending on the sign of the curvature of the wave front. In our case, where the position of the sample is beyond the focusing lens and the beam waist, the wave front curvature of the incident Gaussian beam is positive and the motion of spiral arms is outwards [Fig. 4(b)].

The spiral pattern can be understood as a "bent" stripe pattern whose "arms" are continually driven out by the positive radially symmetric phase gradient. Correspondingly, we find the spirals in the existence range of stripe patterns (Fig. 5). The outermost period of the spiral arms breaks up into

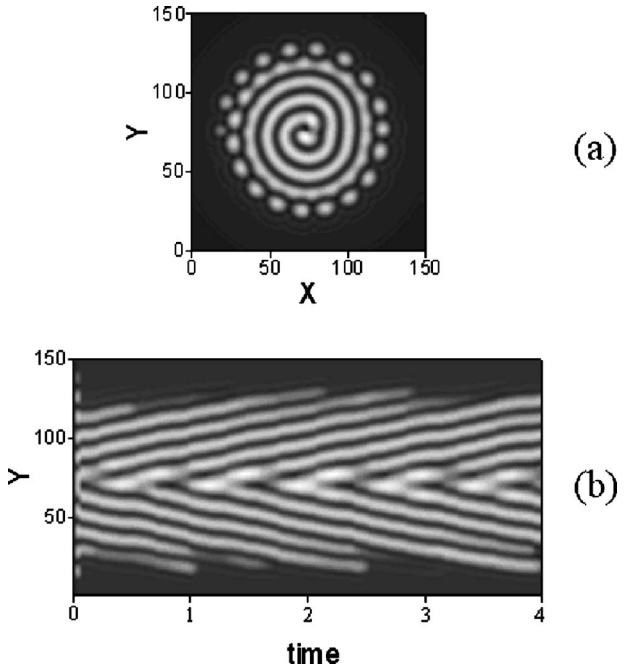

FIG. 4. "Out"-rotation of spiral (numerical simulation): (a) intensity distribution (snapshot), and (b) space-time plot across the spiral illustrating radial motion. X,Y are transverse coordinates in μm. Time is given in μs. Radius of wave front curvature: $R_s=48$ mm. Parameters: $E_s=0.32$, $W_s=200$ μm, and $\theta=-1.5$.

bright solitons [Fig. 4(a)]. These solitons appear since the intensity at the edge of Gaussian beam is smaller than at the center. At the edge the intensity lies already within the existence range of bright solitons (Fig. 5). This figure shows also

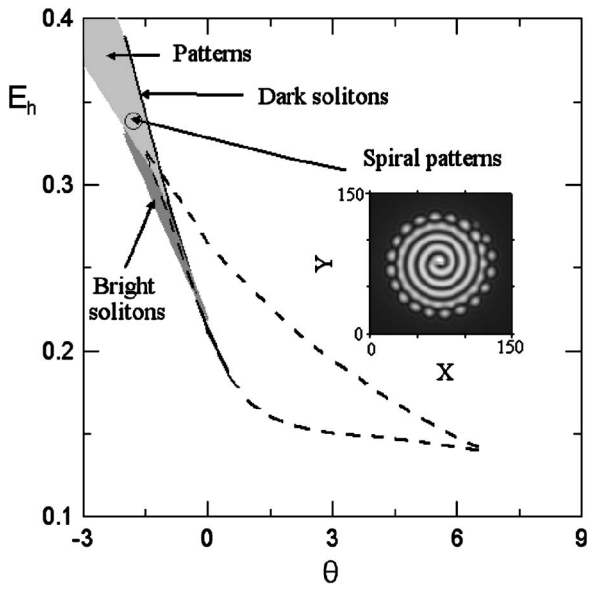

FIG. 5. Phase diagram of numerical stationary solutions of Eq. (1) for mixed dispersive and saturable absorption nonlinearity. Area limited by the dashed line is the plane wave bistability domain. Shaded areas are domains of stability for bright/dark solitons and patterns. Inset shows a spiral pattern in the area marked with a circle.

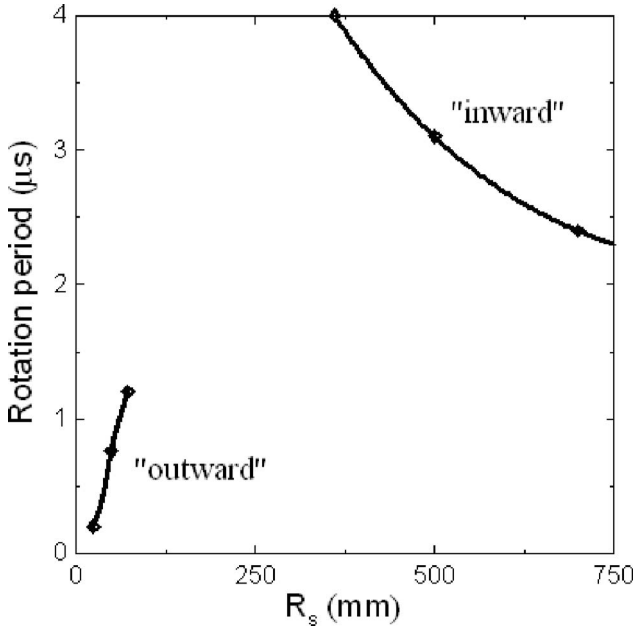

FIG. 6. Calculated dependence of spiral rotation period on radius R of wave front curvature (points correspond to data in Table I). Parameters: $E_s=0.32$, $W_s=200$ μm, and $\theta=-1.5$.

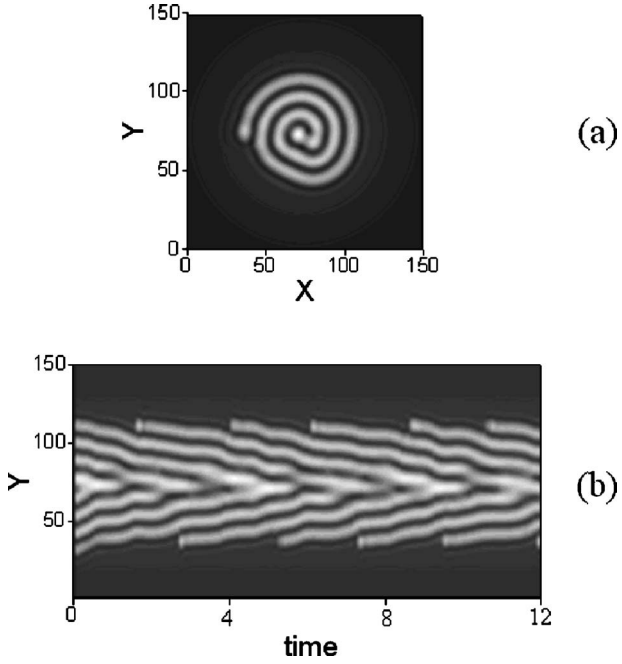

FIG. 7. Snapshot (a) and space-time plot (b) of an "in"-rotating spiral pattern for relative small phase curvature $R_s=700$ mm. X,Y are transverse coordinates in μm. Time is given in μs. Parameters: $E_s=0.32$, $W_s=200$ μm, and $\theta=-1.5$.

that, changing parameters (for instance, detuning), a transition from patterns to spirals can occur as in the experiment (Fig. 3).

The positive phase gradient causes spiral arms to move from the center of the beam to its periphery. The rotation period of the spiral motion is of the order of microseconds and the speed of rotation depends, among other parameter dependences (like diffusion coefficient and relaxation rates), on the radius of wave front curvature (Fig. 6).

The influence of the phase gradient is intuitively understandable. In a fluid picture of nonlinear resonators [3] phase gradient corresponds to flow velocity. Thus the speed of outward motion is directly proportional to the phase gradient. Intensity gradients correspond to pressure gradients through a complicated "compressibility" [3], therefore its influence as well as the influence of other parameters (diffusion coefficient, relaxation rates) is less intuitively clear.

The amplitude radius of the Gaussian beam on the sample is kept constant while the wave front curvature radius is varied. Spirals rotate "out" for relative small radii of wave front curvature [the corresponding temporal dynamics and parameters are given in Fig. 4(b)]. It is intuitively clear that the rotation period should increase with increasing wave front radius (i.e., with decreasing phase gradients, see left part of Fig. 6). Spirals rotating "out" are found in the wave front radius interval from 20 to 80 mm with a rotation period of $0.2-1.2$ μs, respectively. The spiral rotation slows down and the spirals become unstable with increasing R_s. There is also an upper limit for the rotation speed at which the spirals become unstable (rotation period ~ 0.17 μs).

"In"-rotating spirals can be observed if the wave front curvature radius of the exciting beam is large enough (>300 mm, see right part of Fig. 6). In this case, the phase gradient is small and the "in"-rotation is caused by the amplitude gradient (Fig. 7). With decreasing phase gradient (increasing the wave front curvature radius) the "out"-rotation caused by the phase gradients is slowed and can be compensated by "in"-rotation caused by the amplitude gradients. Due to this compensation the spirals do not exist in a certain interval between "out"- and "in"-rotation (center of Fig. 6). Further decreasing the phase gradient, the behavior of "in"-rotation becomes first quasiperiodic. The periodicity is then destroyed and spirals become unstable. For the conditions of Fig. 6 the "in"-rotation curve corresponds mostly to the range of sample positions inside the diffraction (Rayleigh-) length. The "out"-rotation curve corresponds to the beam parameters on the sample for positions beyond the diffraction length. It is interesting to note that the "in"-rotating spirals (Fig. 7) are not symmetric. This may be due to the bright spots in the center of the spiral, which break the spiral symmetry.

It is possible to keep the spiral patterns stable for different positive wave front curvatures by adjusting the radius of the Gaussian beam intensity distribution. At smaller beam radius the amplitude gradient is larger which causes the spirals to rotate inward. Increasing curvature (i.e., decreasing the wave front radius) favors "out"-rotation and can thus compensate the effect of an amplitude gradient. Therefore there is an influence of both the intensity distribution and phase distribution (or wave front curvature) on the spiral patterns.

The calculated spirals show in general several periods of spiral arms [Figs. 4(a), 7(a), and 8(a)], whereas experimentally we observe hardly more than one period (Figs. 2 and 3). It appears that the latter is a consequence of the narrow Gaussian beam (of 45 μm diameter) used in the experiment. To compare with experimental parameters, we look at the

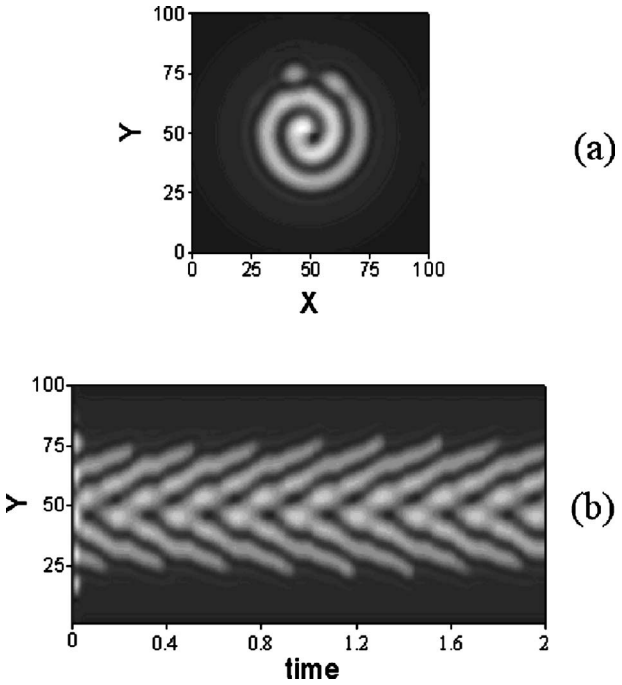

FIG. 8. Snapshot (a) and space-time plot (b) of spiral pattern calculated theoretically for relative small amplitude radius W_s $=80$ μm. X,Y are transverse coordinates in μm. Time is given in μs. Parameters: $E_s=0.33$, $R_s=7.58$ mm, and $\theta=-1.5$.

spiral existence if the amplitude radius of the exciting beam at the beam waist is approximately 25 μm (amplitude radius on the sample $W_s=80$ μm). We have found only "out"-rotating spirals (of little more than one period as in the experiment, Fig. 8) under these conditions, which correspond to a sample position $\sim$7 mm beyond the beam waist. This is beyond the diffraction length of 2.25 mm. The spirals become unstable already for a wave front curvature radius of 8 mm and the corresponding largest rotation period of 0.32 μs (Fig. 9). Table I gives the speed and direction of rotation with the corresponding parameters.

The difference between the ranges of wave front curvature, in which spiral patterns are stable, calculated theoretically, and found experimentally is not unexpected because many parameters (such as carrier recombination time, diffusion coefficient, and susceptibility) are not well known for the sample material, so that we can only expect qualitative equivalences.

In the experiment we could not see a clear rotation of spirals. The reason may be the presence of defects in the sample, "pinning" the spirals as it happens for solitons in this system and/or the large radius of wave front curvature at which the spirals are almost stationary during the illumination time of a few microseconds (Fig. 6). Also, in the theoretical calculations we have not taken into account thermal effects which, indeed, influence the spiral formation and their motion.

At negative wave front curvature the spirals are found to be unstable. This explains why experimentally spirals at positions of the sample between the focusing lens and the beam waist were not found.

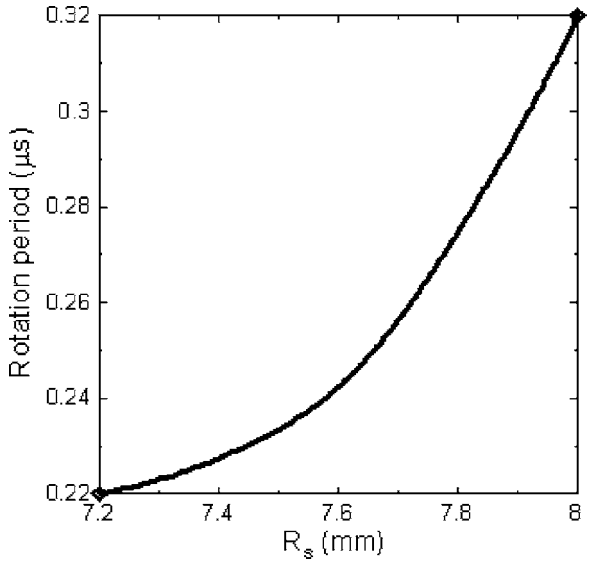

FIG. 9. Rotation period of spiral pattern calculated theoretically in dependence on the radius R of phase curvature for a small amplitude radius of illuminating beam $W_s=80$ μm (points correspond to data in Table I). Parameters: $E_s=0.33$ and $\theta=-1.5$.

IV. CONCLUSION

In this paper the existence of intensity spiral patterns in a multiple quantum well microresonator has been experimentally shown and qualitatively similarly found by simulations. As opposed to other cases of intensity spiral patterns, like those predicted in an internally pumped optical parametric oscillator [1], where the exciting field has no gradients, or the single-mirror feedback system [2], where a nonlinear phase gradient induced by the intensity profile of the pump beam (without linear phase gradient) is sufficient for intensity spiral formation, the spiral formation, in our case, is determined by both pump profile (amplitude gradient) and

TABLE I. The speed and direction of rotation with parameters, corresponding to points on curves from Figs. 6 and 9 where stable spirals are predicted. l_s is the distance from the beam waist to the sample, E_0 is the amplitude of the Gaussian beam in the beam waist (behind the last lens), and W_0 is the radius of the illuminating light amplitude at the beam waist. Other parameters are given in the text.

l_s (mm)	E_0	E_s	W_0 (μm)	W_s (μm)	R_s (mm)	Rotation period (μs)	Direction of rotation
23.3	1.9	0.32	33.2	200	24	0.2	Outward
43	1	0.32	63.8	200	48	0.76	Outward
57.5	0.7	0.32	90	200	72	1.2	Outward
49	0.34	0.32	186	200	360	4	Inward
37.8	0.33	0.32	192	200	500	3.1	Inward
28	0.33	0.32	196	200	700	2.4	Inward
6.6	1.11	0.33	24	80	7.2	0.22	Outward
7.1	0.96	0.33	26.5	80	8	0.32	Outward

linear phase gradient. Interplay of the wave front curvature and the amplitude distribution of the illuminating Gaussian beam appears to be decisive for the rotation and stability of intensity spiral patterns.

ACKNOWLEDGMENTS

U. Peschel, T. Ackemann, and C.O. Weiss are gratefully acknowledged for their moral support. Ye.L. acknowledges the financial support of the Humboldt Foundation.

[1] P. Lodahl, M. Bache, and M. Saffman, Phys. Rev. Lett. **85**, 4506 (2000).
[2] F. Huneus, B. Schäpers, T. Ackemann, and W. Lange, Appl. Phys. B: Lasers Opt. **76**, 191 (2003).
[3] K. Staliunas, Phys. Rev. A **48**, 1573 (1993).
[4] B. G. Sfez *et al.*, Appl. Phys. Lett. **57**, 1849 (1990); I. Abram *et al.*, *ibid.* **65**, 2516 (1994).
[5] X. Hachair *et al.*, Phys. Rev. A **69**, 043817 (2004).
[6] V. B. Taranenko, I. Ganne, R. Kuszelewicz, and C. O. Weiss, Appl. Phys. B: Lasers Opt. **72**, 377 (2001).
[7] S. Barland, J. R. Tredicce, M. Brambilla, L. A. Lugiato, S. Balle, M. Giudici, T. Maggipinto, L. Spinelli, G. Tissoni, T. Knodel, M. Miller, and R. Jaager, Nature (London) **419**, 699 (2002).
[8] R. Kuszelewicz, I. Ganne, I. Sagnes, G. Slekys, and M. Brambilla, Phys. Rev. Lett. **84**, 6006 (2000).
[9] V. B. Taranenko and C. O. Weiss, IEEE J. Sel. Top. Quantum Electron. **8**, 488 (2002).
[10] A. J. Scroggie, J. M. McSloy, and W. J. Firth, Phys. Rev. E **66**, 036607 (2002).
[11] V. B. Taranenko, C. O. Weiss, and B. Schapers, Phys. Rev. A **65**, 013812 (2002).
[12] M. Haelterman and G. Vitrant, J. Opt. Soc. Am. B **9**, 1563 (1992).
[13] G. Grynberg, Opt. Commun. **109**, 483 (1994).